Supporting Information

Contribution of Biomass Burning to Ambient Particulate Polycyclic Aromatic Hydrocarbons at a Regional Background Site in East China

Shuduan Mao[†,‡], Jun Li [†], Zhineng Cheng [†], Guangcai Zhong [†], Kechang Li [†], Xiang Liu [†], and Gan Zhang [*,†]

[†] State Key Laboratory of Organic Geochemistry, Guangzhou Institute of Geochemistry, Chinese Academy of Sciences, Guangzhou 510640, China;

[‡] University of Chinese Academy of Sciences, Beijing 100049, China.

*Corresponding to: zhanggan@gig.ac.cn

List of the Supporting Information:

Figure S1. Clustered mean five-day trajectories reaching the sampling site at NAEO for the campaign period during four seasons.

Figure S2. Temporal variations of particulate PAHs, anhydrosugars, OC, and EC collected from August 2012 to August 2015 at NAEO.

Figure S3. Wild fire counts detected by MODIS on NASA satellites from 2012 to 2015.

Figure S4. Five-day air mass backward trajectories for selected samples in summer.

Figure S5. Normalized congener patterns of the four factor profiles from PMF analysis and the contributions of each factor to PAHs.

Text S1. Sample pretreatments and analysis

Sample pretreatments

PAHs: A section (10 cm×12.7 cm) of each filter sample was spiked with 1000 ng perdeuterated PAHs as surrogates and extracted in Soxhlets for 24 h with dichloromethane (DCM). The extracts were then concentrated using a rotary evaporator and solvent-exchanged into hexane with a volume of 0.5mL. Purification procedures were performed with column chromatography, in which anhydrous sodium sulfate (1 cm), neutral silica gel (3cm, 3% deactivated) and neutral alumina (3 cm, 3% deactivated) were contained. The PAH fractions were eluted with 15 mL of a mixture of hexane and DCM (1:1 by volume). The eluent solvent was then concentrated under a gentle nitrogen stream to a final volume of 0.5mL. Befor analysis, 1000ng of hexamethylbenzene (Aldrich Chemical, Gillingham, Dorset, USA) was added as an internal standard.

Anhydrosugars: A section (15.9cm^2) of each filter sample was spiked with 1000 ng ^{13}C-labeled levoglucosan (lev) as recovery standard and then extracted in Soxhlets for 24 h with a mixture of DCM and Methanol (40:3 by volume). The extracts were anhydrated with anhydrous sodium sulfate column and then concentrated using a rotary evaporator with a volume of 0.5mL. Afterward, the concentrates were transferred into vials, spiked with 1000 ng methyl β-L-xylanopyranoside (m-XP) as an internal standard, and then dried completely in a gentile nitrogen stream. Finally, 300 μL derivatization reagent [(200 μL *N,O*-Bis-(trimethylsilyl) trifluoroacetamide (BSTFA) with 1% trimethylsilyl chloride and 100μL pyridine)] was added for the sequent reaction at 70°C for 1h.

Instrumental analysis

The PAHs were analyzed on an Agilent 7890 gas chromatograph equipped with a DB-5MS capillary column (30 m×0.25 mm× 0.25 μm; Agilent, USA) and a mass spectrometer (MSD, Agilent

5975). 1 μL of each extract was injected in splitless and operated under electron ion source (-70 eV) in selective ion monitoring (SIM) mode with a 9 min solvent delay time. High purity helium was used as the carrier gas at a flow rate of 1.2 ml/min. The temperature of transfer line, injector interface and ion source were set at 280°C, 290°C and 230°C, respectively. The initial oven temperature was set at 60°C for 1 min, then raised to 100°C at a rate of 4°C/ min, to 295°C at 10°C/ min, and hold for 20 min. 16 USEPA priority PAHs were quantified: naphthalene (Nap), acenaphthene(Ace), acenaphthylene (Acy), fluorene (Flu), phenanthrene (Phe), anthracene (Ant), fluoranthene (Fla), pyrene (Pyr), benzo[a]anthracene (BaA), chrysene (Chr), benzo[b]fluoranthene (BbF), benzo[k]fluoranthene (BkF), benzo[a]pyrene (BaP), dibenzo[a,h]anthracene (DahA), benzo[g,h,i]perylene (BghiP) and indeno[1,2,3-c,d]pyrene (IcdP). However, the concentration of Nap is not reported in this study because of relatively low recovery due to evaporative losses during chemical analysis.

All the PAH data were corrected by the recovery of the surrogate standards. Acenaphthene-d_{10} was used to correct the recovery of the Ace, Acy and Flu; phenanthrene-d_{10} was used to correct the recovery of the Phe, Ant, Fla and Pyr; chrysene-d_{12} was used to correct the recovery of the BaA and Chr; and perylene-d_{12} was used to correct the recovery of the 5- and 6- ring PAHs.

Anhydrosugars were also analyzed on Agilent 7890/5975 GC-MS with a DB-5MS capillary column (30 m×0.25 mm× 0.25 μm; Agilent, USA). The GC oven temperature was set at 65 °C for 2 min, then 4°C /min to 290 °C, and hold for 20 min. The Other settings were the same with PAHs analysis.

A punch (1 cm^2) of each filter was analyzed for organic carbon (OC) and elemental carbon (EC) with a Desert Research Institute (DRI) model 2015 Thermal/Optical Carbon Analyzer (Atmoslytic Inc., Calabasas, CA). IMPROVE_A (Interagency Monitoring of Protected Visual Environment)

temperature protocol was implemented. This protocol yielded four OC fractions (OC1, OC2, OC3, and OC4 at 140°C, 280°C, 480°C and 580°C, respectively, in an insert helium environment), one pyrolyzed carbon (OP) fraction (determined when the reflected laser light attained its original intensity after O_2 was added to the combustion atmosphere), and three EC fractions (EC1, EC2, and EC3 at 580°C, 740°C and 840°C, in an oxidizing 2% O_2/ 98% He environment). The IMPROVE_A protocol defines total carbon (TC) as OC + EC, OC as OC1 + OC2 + OC3 + OC4 + OP, and EC as EC1 + EC2 + EC3 – OP.

Text S2. Positive matrix factorization (PMF) modeling

PMF has often been used for the source apportionment of pollutants in atmospheric aerosols. The detailed concept and application of PMF source apportionment is described in the EPA PMF 5.0 Fundamentals & User Guide (www.epa.gov/heasd/products/pmf). Prior to the analysis, any undetectable values (null values) were replaced with values of one half the method detection limits (MDLs). An uncertainty of 20% for each PAH dataset, and 10% for lev, were adopted based on the repeated analysis of a standard reference material.[1-3] Considering that Ace, Acy, and Flu were below the MDLs in nearly half samples, and the average percentages of these three species were less than 0.4% of Σ_{15}PAHs, they were thus not included in the PMF model.

During the PMF analysis, a 73 × 13 (73 samples with other 12 selected PAHs and lev) data set was introduced and four factors were adopted baced on the *Q* values. However, a fraction of levo will be shifted to secondary source because of ageing process, leading to underestimation of the contribution of biomass burning.[4] To minimize the underestimation, constraint was exerted by setting levo to zero in sources except for biomass burning. Figure S5 showed the source contribution distributions of individual factors after applying constraint. Each factor profile was then identified by comparison to the source profiles.

Factor 1 was characterized by an overwhelmingly high loading of lev, which is widely used as a biomass burning tracer. Factor 1 was therefore used to represent biomass burning.

Factor 2 had high loadings of BghiP, IcdP, and BbF. IcdP and BghiP are used as indicators of vehicular emissions.[5, 6] Moreover, the concentration ratios of IcdP/(IcdP+BghiP) and BaA/(BaA+Chr) were 0.44 and 0.40, respectively, which were within the typical ranges of vehicular emissions and petroleum combustion [IcdP/(IcdP+BghiP):0.2-0.5; BaA/(BaA+Chr): >0.35].[7] Therefore, factor 2 was

attributed to vehicular emissions, with oil and diesel used as fuel.

Factor 3 was highly loaded with Fla and Pyr, and moderately loaded with Phe, Chr, Bap, and DahA. Flu and Pyr have been considered to be markers of coal combustion.[6, 8] This factor has the same profile with previous report by Wang *et al*.[8] Additionally, the concentration ratios of Fla/(Fla+Pry) and BaA/(BaA+Chr) were 0.53 and 0.26, respectively. These values were within the typical ranges for wood and coal combustion [Fla/(Fla+Pry): >0.5; BaA/(BaA+Chr): 0.2-0.35].[7, 9] Because factor 3 has scarce loading of lev and biomass burning was attributed to factor 1 due to the high loading of lev, factor 3 was thus characterized as coal combustion.

Factor 4 was predominantly composed of Ant and Phe. This profile contained more volatile PAHs and represented the fugitive loss of petroleum products.[1, 10] Low molecular weight PAHs are more likely to evaporate from water and soil to the atmosphere. Air-sea exchange could therefore be a potential source of these PAHs, especially during warm periods.[11-13] The concentration ratio of Ant/(Ant+Phe) was less than 0.1 for this factor, indcating that it was a petroleum residue source.[7, 9] Consequently, factor 4 was attributed to volatilization, and included oil leakage from vehicles and ships, or revolatilization directly from seawater, soil, and ground surfaces.

Table S1. Method detection limits of fifteen particulate PAHs, three anhydrosugars, OC, and EC

Compounds	Method detection limit (MDL)	Compounds	Method detection limit (MDL)
Acy	1.7 pg/m^3	BkF	1.08 pg/m^3
Ace	5.2 pg/m^3	BaP	0.94 pg/m^3
Flu	5.88 pg/m^3	IcdP	2.08 pg/m^3
Phe	19.39 pg/m^3	DahA	1.58 pg/m^3
Ant	1.16 pg/m^3	BghiP	2.03 pg/m^3
Fla	4.54 pg/m^3	levoglucosan	29.5 ng/m^3
Pry	7.08 pg/m^3	galactosan	2 ng/m^3
BaA	7.57 pg/m^3	mannosan	5.15 ng/m^3
Chr	3.62 pg/m^3	OC	81.31 ng/m^3
BbF	2.1 pg/m^3	EC	0

Table S2. Average concentrations and ranges of fifteen particulate PAHs, three anhydrosugars, OC, and EC

Compounds	Mean [a] ± SD [b]	Range	Median	NAD [c]
Particlate PAHs, ng/m^3				
Acy	0.02±0.02	BDL [d]-0.12	0.01	43
Ace	0.01±0.01	BDL-0.03	BDL	28
Flu	0.03±0.04	BDL-0.17	0.02	42
Phe	0.37±0.54	BDL-2.27	0.13	56
Ant	0.02±0.02	BDL-0.09	0.01	60
Fla	0.96±1.30	0.01-4.91	0.34	73
Pyr	0.72±0.93	BDL-3.53	0.35	67
BaA	0.21±0.30	BDL-1.54	0.07	58
Chr	0.46±0.67	BDL-3.90	0.15	70
BbF	1.16±1.60	0.003-8.51	0.43	73
BkF	0.30±0.41	0.002-2.30	0.10	73
BaP	0.30±0.42	BDL-2.08	0.10	71
IcdP	0.58±0.85	BDL-4.51	0.19	72
DahA	0.07±0.11	BDL-0.60	0.02	61
BghiP	0.64±0.89	0.003-4.73	0.21	73
Σ15PAHs	5.84±7.82	0.01-38.59	2.25	73
Anhydrosugars, ng/m^3				
levoglucosan	51.71±84.37	BDL-493.14	13.03	60
galactosan	1.96±2.86	BDL-13.06	0.61	52
mannosan	3.13±4.08	BDL-16.42	1.18	52
OC, EC， ug/m^3				
OC	5.91±5.10	0.28-24.52	4.68	73
EC	1.79±1.76	BDL-11.44	1.27	72

[a]. Mean: arithmetic mean.

[b]. SD: standard deviation.

[c]. NAD: number above detection limit.

[d]. BDL: below the method detection limit.

Table S3. Average concentrations of particulate Σ15PAHs, three anhydrosugars, OC, and EC in different seasons

Seasons	**Spring ave. (range)**	**Summer ave. (range)**	**Fall ave. (range)**	**Winter ave. (range)**
Sampling time	Mar., Apr., May	Jun., Jul., Aug.	Sep., Oct., Nov.	Dec., Jan., Feb.
Number of data	17	21	17	18
Levoglucosan, ng/m^3	19.07±15.49 (BDL-56.39)	3.69±4.07 (BDL-13.03)	73.67±120.8 (BDL-493.142)	117.84±84.49 (BDL-369.86)
Galactosan, ng/m^3	0.82±0.90 (BDL-3.72)	0.11±0.17 (BDL-0.45)	2.17±3.17 (BDL-13.06)	5.00±3.01 (BDL-12.81)
Mannosan, ng/m^3	1.71±1.98 (BDL-8.73)	0.23±0.35 (BDL-0.90)	3.24±4.04 (BDL-15.85)	7.73±4.08 (BDL-16.42)
Σ15PAHs, ng/m^3	2.81±2.32 (0.14-7.63)	0.42±0.39 (0.04-1.54)	4.48±4.27 (0.01-13.90)	16.30±8.59 (2.15-38.59)
OC, μg/m^3	4.45±2.87 (0.37-8.92)	2.38±1.71 (0.28-6.44)	7.18±5.74 (0.31-24.52)	10.21±5.41 (2.09-23.00)
EC, μg/m^3	1.19±0.56 (0.39-2.10)	0.72±0.42 (0.03-1.45)	2.05±1.63 (BDL-6.83)	3.35±2.39 (0.51-11.44)

Table S4. Emission inventory of particulate PAHs and three anhydrosugars for different types of biomass burning

	Types	Man/Gal	Lev/Man	Phe/Lev, 10^{-3}	Ant/Lev, 10^{-3}	Fla/Lev, 10^{-3}	Pry/Lev, 10^{-3}	BaA/Lev, 10^{-3}	Chr/Lev, 10^{-3}	BbF/Lev, 10^{-3}	BkF/Lev, 10^{-3}	BaP/Lev, 10^{-3}	IcdP/Lev, 10^{-3}	DahA/Lev, 10^{-3}	BghiP/Lev, 10^{-3}	Ref.
Hardwoods	red maple	-	33.02	0.80	0.17	2.90	3.90	1.84	2.32	1.21	1.22	1.14	1.51	0.06	0.61	14
	northern red oak	1.35	35.46	0.20	0.06	1.09	1.33	0.52	0.64	0.21	0.29	0.33	0.23	0.02	0.15	14
	Yellow Poplar	5.01	10.67	0.22	0.04	1.62	1.93	0.79	0.90	0.40	0.44	0.54	0.38	0.03	0.27	15
	White Ash	-	12.88	-	0.20	2.95	3.88	1.90	1.94	1.24	1.37	1.62	1.27	0.09	0.76	15
	Sweet-gum	-	18.38	-	0.08	-	-	0.77	0.94	0.55	0.52	0.59	0.48	0.04	0.24	15
	Mockernut Hickory	1.82	24.73	0.23	0.05	1.75	2.00	0.88	0.93	0.44	0.52	0.64	0.42	0.04	0.31	15
	musasa	1.10	22.73	2.60	0.48	0.64	0.68	0.78	0.48	0.80	0.46	1.22	0.54	0.09	0.38	16
	Average	**2.32±1.82**	**22.55±9.43**	**0.81±1.03**	**0.15±0.16**	**1.83±0.94**	**2.29±1.33**	**1.07±0.56**	**1.16±0.69**	**0.69±0.40**	**0.69±0.42**	**0.87±0.46**	**0.69±0.49**	**0.05±0.03**	**0.39±0.22**	
Softwoods	eastern white pine	6.98	5.81	3.00	0.61	19.87	17.12	4.76	4.70	3.00	3.55	3.38	2.43	0.21	1.34	14
	eastern hemlock	10.34	3.73	0.76	0.22	3.90	4.20	1.76	1.84	0.69	0.88	0.95	0.67	0.04	0.37	14
	balsam fir	6.74	4.68	0.90	0.26	3.51	3.81	1.56	1.73	0.61	0.80	0.86	0.65	0.06	0.38	14
	Loblolly Pine	-	4.53	11.00	1.81	17.62	16.36	5.00	5.06	2.09	2.91	3.05	2.56	0.22	1.24	15
	Slash Pine	-	4.91	2.47	0.85	18.49	17.64	3.28	4.09	2.11	1.81	1.96	2.49	0.19	1.00	15
	pine	1.33	3.75	0.13	0.02	0.05	0.05	0.08	0.07	0.09	0.03	0.09	0.04	0.01	0.02	16
	pine and green needles	0.87	6.54	1.65	0.48	1.29	1.65	0.44	-	0.47	0.75	1.18	0.31	0.05	0.21	16
	spruce and green needles	3.00	4.71	0.30	0.05	0.08	0.09	0.23	0.19	0.34	0.11	0.36	0.23	0.05	0.18	16
	Conifer vegetation	2.36	2.17	4.95	0.99	4.62	4.29	1.98	2.20	3.74		1.76	1.10	-	1.32	17
	High desert Juniper	0.88	5.37	2.96	0.05	3.51	3.61	0.74	1.24	0.99		0.79	0.00	-	0.00	17
	Ponderosa pine	1.80	3.52	3.16	0.79	3.02	3.02	1.19	1.83	2.42		0.89	0.00	-	0.00	17
	Lodgepole pine	1.36	3.59	4.09	0.98	4.28	4.61	1.26	1.81	2.28		0.37	0.00	-	0.00	17
	Average	**3.57±3.28**	**4.44±1.18**	**2.95±2.95**	**0.59±0.53**	**6.69±7.39**	**6.37±6.62**	**1.86±1.66**	**2.25±1.68**	**1.57±1.19**	**1.36±1.29**	**1.30±1.04**	**0.87±1.03**	**0.10±0.09**	**0.51±0.55**	
Annual Plant	Rice straw(California)	-	-	0.25	0.06	0.54	0.49	0.34	0.30	0.22	0.16	0.27	0.14	0.02	0.13	18
	Wheat straw(Washington)	-	-	0.20	0.06	1.24	1.25	1.60	1.61	1.23	1.24	1.63	0.97	0.12	0.97	18

Rice straw(Japan)	-	-	-	-	0.94	1.06	0.65	0.76	0.59	0.46	0.54	0.39	0.05	0.36	[19]
Barley straw	-	-	0.15	-	2.91	3.64	2.38	2.72	1.59	1.72	1.99	1.46	0.18	1.32	[19]
savanna grass	0.70	21.74	0.52	0.15	0.50	0.60	0.30	-	0.36	0.56	1.00	0.22	0.04	0.16	[16]
Wheat (Washington)	-	-	-	-	0.93	1.20	4.07	1.67	3.13	3.40	1.87	0.21	0.80	0.55	[20]
Kentucky bluegrass	-	-	-	-	2.31	2.17	3.14	1.49	0.89	1.26	1.20	0.15	0.40	0.54	[20]
Rice straw	0.57	30.65	-	-	-	-	-	-	-	-	-	-	-	-	[21]
Agricultural waste	0.50	26.00	-	-	-	-	-	-	-	-	-	-	-	-	[22]
Average	**0.59±0.10**	**26.13±4.46**	**0.28±0.17**	**0.09±0.05**	**1.34±0.92**	**1.49±1.10**	**1.78±1.47**	**1.43±0.83**	**1.14±1.00**	**1.26±1.09**	**1.21±0.66**	**0.51±0.51**	**0.23±0.28**	**0.58±0.43**	

Table S5. Decays of individual particulate PAHs cited from the study by Jariyasopit et al. [(the particulate matter-bound PAHs exposed to an average tropospheric OH radical concentration (1.0×10^6 molecule cm^{-3}) for ~6-7 days)] [23]

Individual PAH	Average percent change
Phe	-25% ± 6%
Ant	-40% ± 3%
Fla	-19% ± 3%
Pyr	-24% ± 5%
BaA	-28% ± 3%
Chr	3% ± 10%
BbF	-7% ± 3%
BkF	-9% ± 3%
BaP	-22% ± 8%
IcdP	-5% ± 3%
DahA	-8% ± 3%
BghiP	-11% ± 3%

Table S6. Corrected ratios of individual particulate PAHs to lev [$(PAHs/Lev)^*_{bb}$] based on decay rates of PAHs and lev

The ratio of individual PAH to lev	Corrected value, $\mathbf{10^{-3}}$
Phe/lev	0.76
Ant/lev	0.11
Fla/lev	1.85
Pyr/lev	2.18
BaA/lev	0.96
Chr/lev	1.16
BbF/lev	0.80
BkF/lev	0.78
BaP/lev	0.85
IcdP/lev	0.82
DahA/lev	0.06
BghiP/lev	0.43

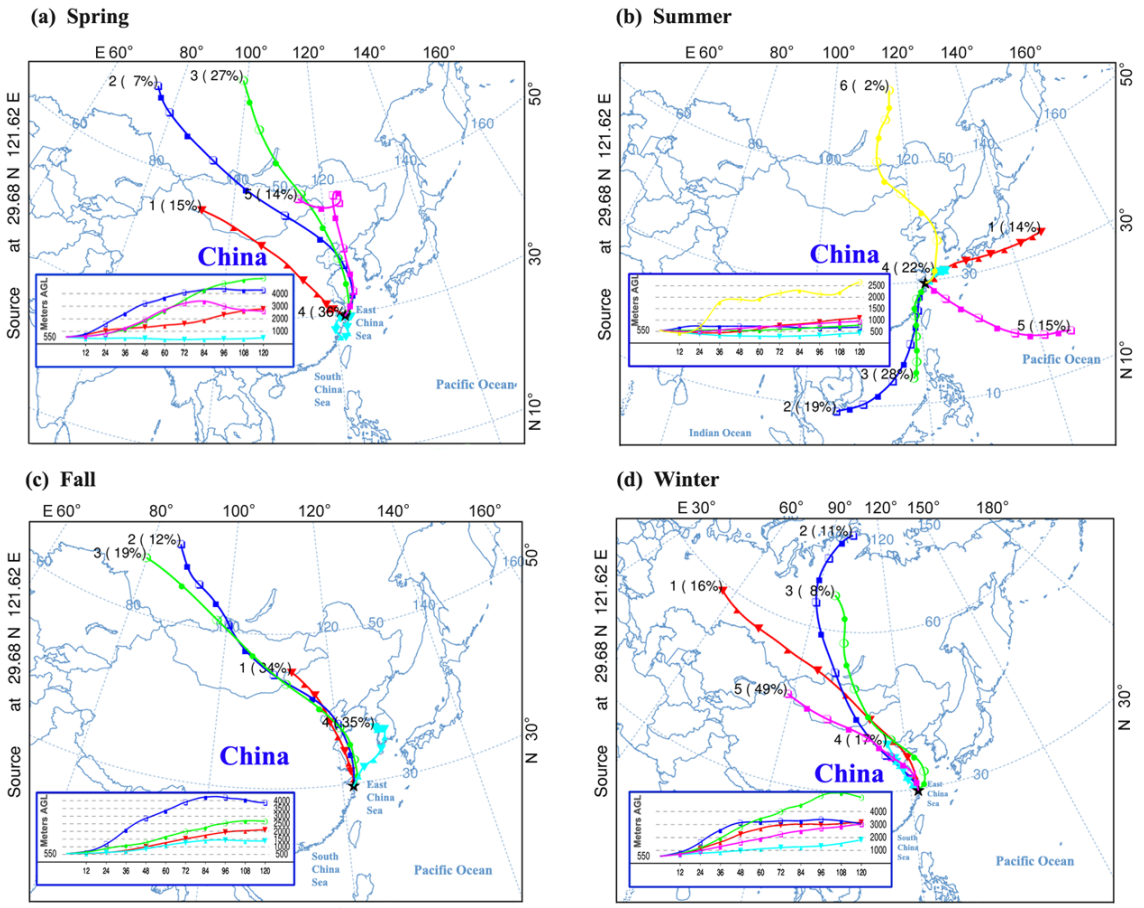

Figure S1. Clustered mean five-day trajectories reaching the sampling site at NAEO for the campaign period during spring (panel a, March, April, and May), summer (panel b, June, July, and August), fall (panel c, September, October, and November), and winter (panel d, December, January, and February) (http://ready.arl.noaa.gov/HYSPLIT.php).

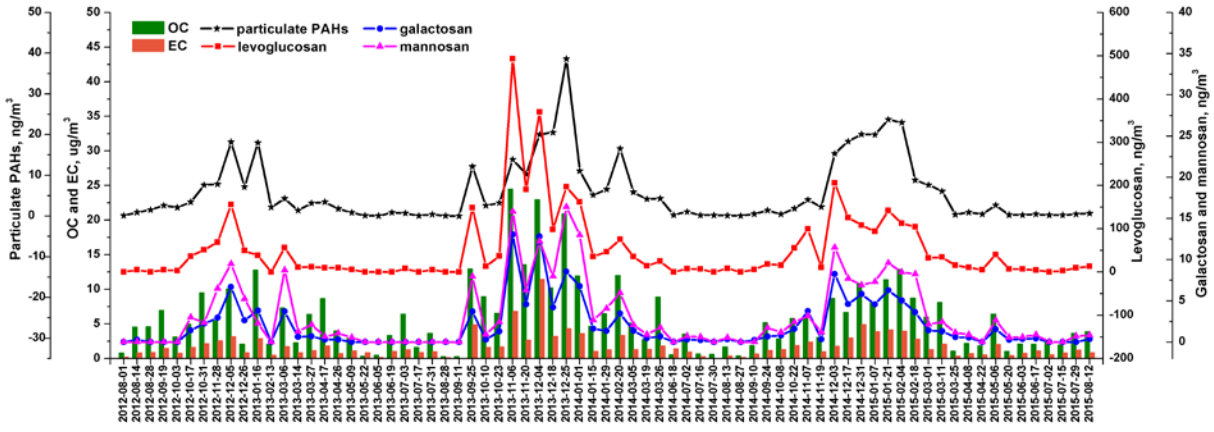

Figure S2. Temporal variations of particulate PAHs, three anhydrosugars, OC, and EC collected from August 2012 to August 2015 at NAEO.

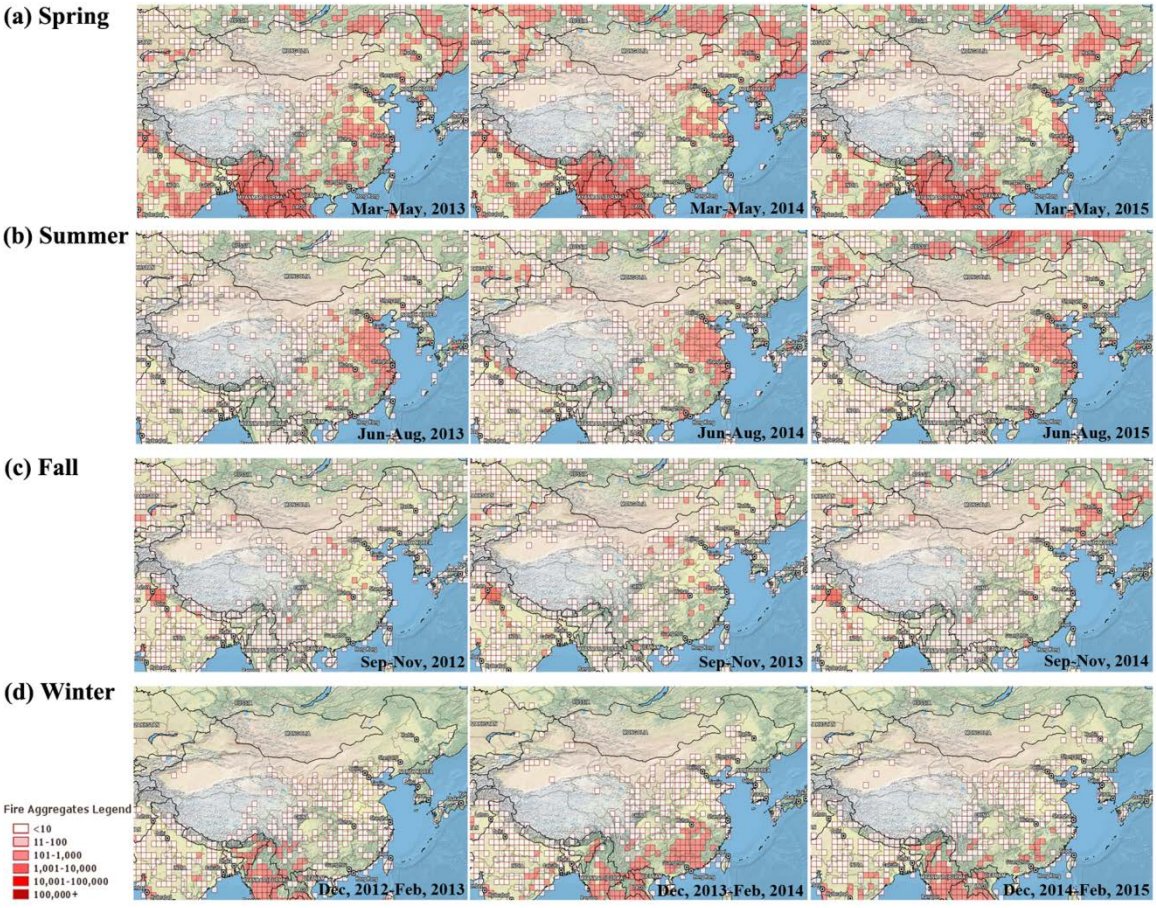

Figure S3. Wild fire counts detected by MODIS on NASA satellites for spring (a), summer (b), fall (c) and winter (d) from 2012 to 2015. (https://firms.modaps.eosdis.nasa.gov/firemap/)

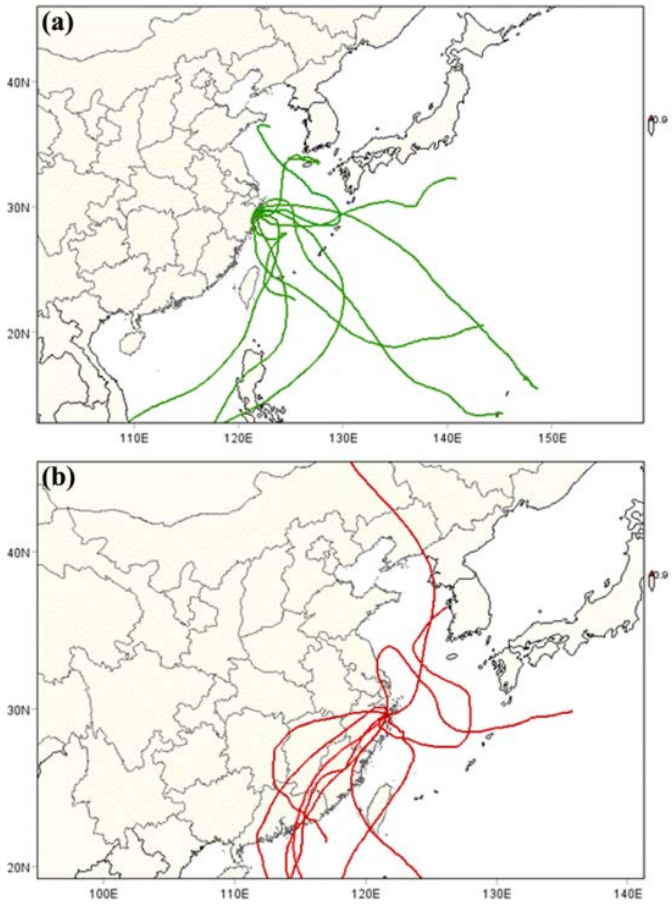

Figure S4. Five-day air mass backward trajectories for selected samples in summer when the concentrations of levoglucoasn were below the MDL (a) and above the MDL (b)

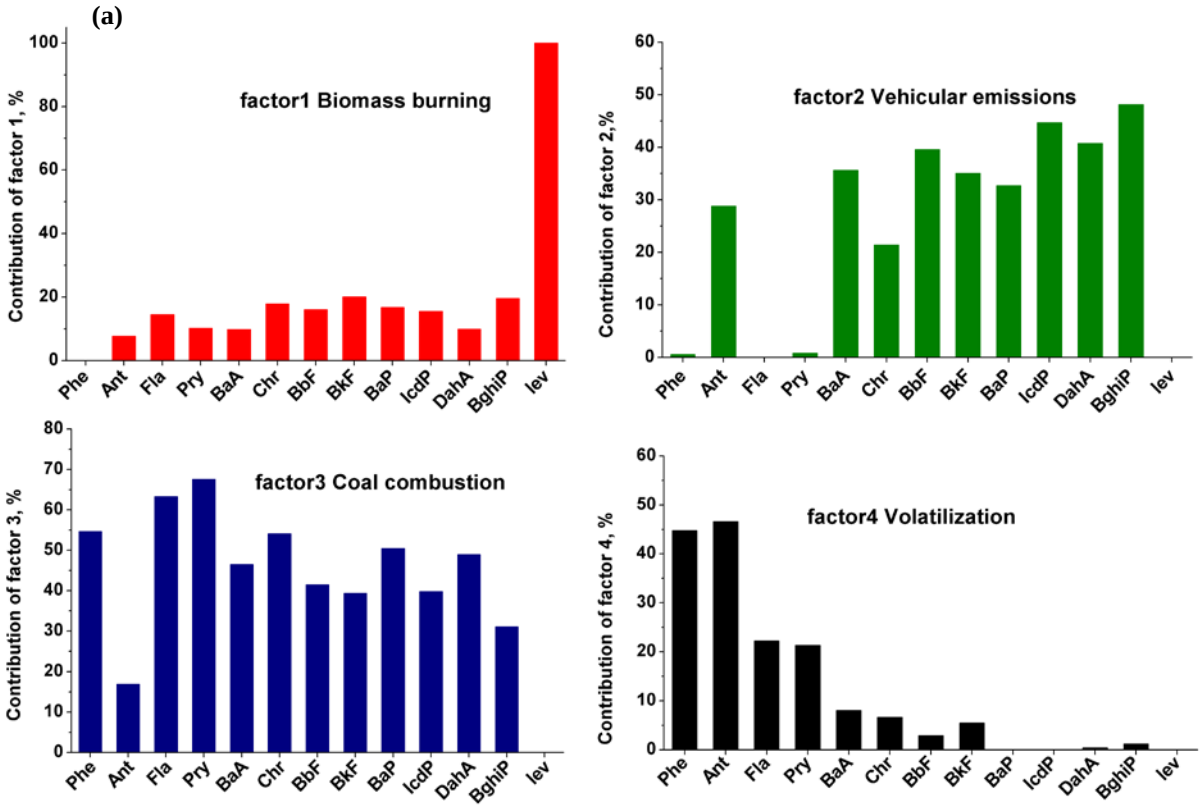

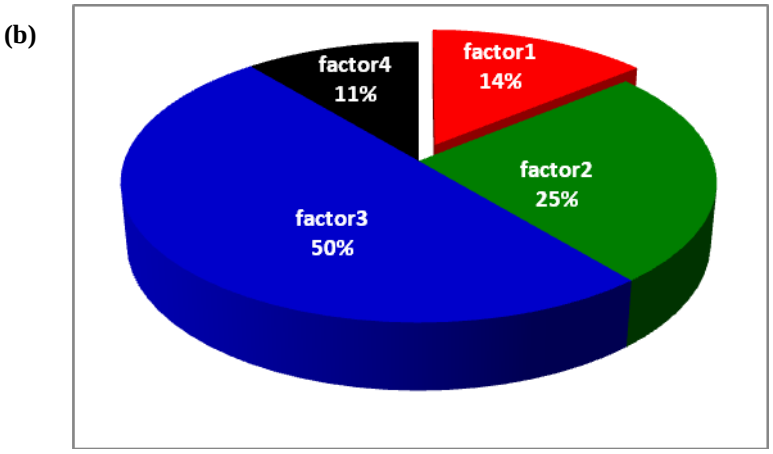

Figure S5. Normalized congener patterns of the four factor profiles from PMF analysis (a) and the contributions of each factor to PAHs (b).

References

(1) Fang, Y.; Chen, Y.; Tian, C.; Lin, T.; Hu, L.; Li, J.; Zhang, G. Application of PMF receptor model merging with PAHs signatures for source apportionment of black carbon in the continental shelf surface sediments of the Bohai and Yellow Seas, China. *J. Geophys. Res.: Oceans* **2016,** *121*, (2), 1346-1359.

(2) Mai, B.; Qi, S.; Zeng, E. Y.; Yang, Q.; Zhang, G.; Fu, J.; Sheng, G.; Peng, P.; Wang, Z. Distribution of Polycyclic Aromatic Hydrocarbons in the Coastal Region off Macao, China: Assessment of Input Sources and Transport Pathways Using Compositional Analysis. *Environ. Sci. Technol.* **2003,** *37*, 4855-4863.

(3) Li, X.; Chen, M.; Le, H. P.; Wang, F.; Guo, Z.; Iinuma, Y.; Chen, J.; Herrmann, H. Atmospheric outflow of $PM_{2.5}$ saccharides from megacity Shanghai to East China Sea: Impact of biological and biomass burning sources. *Atmos. Environ.* **2016,** *143*, 1-14.

(4) Wang, Q. Q.; Huang, X. H. H.; Zhang, T.; Zhang, Q.; Feng, Y.; Yuan, Z.; Wu, D.; Lau, A. K. H.; Yu, J. Z. Organic tracer-based source analysis of PM $_{2.5}$ organic and elemental carbon: A case study at Dongguan in the Pearl River Delta, China. *Atmos. Environ.* **2015,** *118*, 164-175.

(5) Lin, T.; Hu, L.; Guo, Z.; Qin, Y.; Yang, Z.; Zhang, G.; Zheng, M. Sources of polycyclic aromatic hydrocarbons to sediments of the Bohai and Yellow Seas in East Asia. *J. Geophys. Res.: Atmos.* **2011,** *116*, (D23), D23305.

(6) Harrison, R. M.; Smith, D. J. T.; Luhana, S. Source Apportionment of Atmospheric Polycyclic Aromatic Hydrocarbons Collected from an Urban Location in Birmingham, U.K. *Environ. Sci. Technol.* **1996,** *30*, (3), 825-832.

(7) Tobiszewski, M.; Namiesnik, J. PAH diagnostic ratios for the identification of pollution emission sources. *Environ. Pollut.* **2012,** *162*, 110-119.

(8) Wang, F.; Lin, T.; Li, Y.; Ji, T.; Ma, C.; Guo, Z. Sources of polycyclic aromatic hydrocarbons in $PM_{2.5}$ over the East China Sea, a downwind domain of East Asian continental outflow. *Atmos. Environ.* **2014,** *92*, 484-492.

(9) Katsoyiannis, A.; Sweetman, A. J.; Jones, K. C. PAH molecular diagnostic ratios applied to atmospheric sources: a critical evaluation using two decades of source inventory and air concentration data from the UK. *Environ. Sci. Technol.* **2011,** *45*, (20), 8897-8906.

(10) Zakaria, M. P.; Takada, H.; Tsutsumi, S.; Ohno, K.; Yamada, J.; Kouno, E.; Kumata, H. Distribution of polycyclic aromatic hydrocarbons (PAHs) in rivers and estuaries in Malaysia: A widespread input of petrogenic PAHs. *Environ. Sci. Technol.* **2002,** *36*, (9), 1907-1918.

(11) Cheng, J. O.; Ko, F. C.; Lee, C. L.; Fang, M. D. Air-water exchange fluxes of polycyclic aromatic hydrocarbons in the tropical coast, Taiwan. *Chemosphere* **2013,** *90*, (10), 2614-2622.

(12) Kaya, E.; Dumanoglu, Y.; Kara, M.; Altiok, H.; Bayram, A.; Elbir,T.; Odabasi, M. Spatial and temporal variation and air-soil exchange of atmospheric PAHs and PCBs in an industrial region. *Atmospheric Pollution Research* **2012,** *3*, (4), 435-449.

(13) Degrendele, C.; Audy, O.; Hofman, J.; Kucerik, J.; Kukucka, P.; Mulder, M. D.; Pribylova, P.; Prokes, R.; Sanka, M.; Schaumann, G. E.; et al. Diurnal Variations of Air-Soil Exchange of Semivolatile Organic Compounds (PAHs, PCBs, OCPs, and PBDEs) in a Central European Receptor Area. *Environ. Sci. Technol.* **2016,** *50*, (8), 4278-4288.

(14) Fine, P. M.; Cass, G. R.; Simoneit, B. R. T. Chemical characterization of fine particle emissions from fireplace combustion of woods grown in the Northeastern United States. *Environ. Sci. Technol.* **2001,** *35* (13), 2665-2675.

(15) Fine, P. M.; Cass, G. R.; Simoneit, B. R. T. Chemical characterization of fine particle emissions from the fireplace combustion of woods grown in the Southern United States. *Environ. Sci. Technol.* **2002,** *36* (7), 1442-1451.

(16) Iinuma, Y.; Brüggemann, E.; Gnauk, T.; Müller, K.; Andreae, M. O.; Helas, G.; Parmar, R.; Herrmann, H. Source characterization of biomass burning particles: The combustion of selected European conifers, African hardwood, savanna grass, and German and Indonesian peat. *J. Geophys. Res.: Atmos.* **2007,** *112* (D8), 209.

(17) Medeiros, P. M.; Simoneit, B. R. T. Source profiles of organic compounds emitted upon combustion of green vegetation from temperate climate forests. *Environ. Sci. Technol.* **2008,** *42* (22), 8310-8316.

(18) Hays, M. D.; Fine, P. M.; Geron, C. D.; Kleeman, M. J.; Gullett, B. K. Open burning of agricultural biomass: Physical and chemical properties of particle-phase emissions. *Atmos. Environ.* **2005,** *39* (36), 6747-6764.

(19) Fushimi, A.; Saitoh, K.; Hayashi, K.; Ono, K.; Fujitani, Y.; Villalobos, A. M.; Shelton, B. R.; Takami, A.; Tanabe, K.; Schauer, J. J. Chemical characterization and oxidative potential of particles emitted from open burning of cereal straws and rice husk under flaming and smoldering conditions. *Atmos. Environ.* **2017,** *163*, 118-127.

(20) Dhammapala, R.; Claiborn, C.; Jimenez, J.; Corkill, J.; Gullett, B.; Simpson, C.; Paulsen, M. Emission factors of PAHs, methoxyphenols, levoglucosan, elemental carbon and organic carbon from simulated wheat and Kentucky bluegrass stubble burns. *Atmos. Environ.* **2007,** *41* (12), 2660-2669.

(21) Sullivan, A. P.; Holden, A. S.; Patterson, L. A.; McMeeking, G. R.; Kreidenweis, S. M.; Malm, W. C.; Hao, W. M.; Wold, C. E.; Collett, J. L. A method for smoke marker measurements and its potential application for determining the contribution of biomass burning from wildfires and prescribed fires to ambient $PM_{2.5}$ organic carbon. *J. Geophys. Res.: Atmos.* **2008,** *113* (D22), 302.

(22) Munchak, L. A.; Schichtel, B. A.; Sullivan, A. P.; Holden, A. S.; Kreidenweis, S. M.; Malm, W. C.; Collett, J. L. Development of wildland fire particulate smoke marker to organic carbon emission ratios for the conterminous United States. *Atmos. Environ.* **2011,** *45* (2), 395-403.

(23) Jariyasopit, N.; Zimmermann, K.; Schrlau, J.; Arey, J.; Atkinson, R.; Yu, T. W.; Dashwood, R. H.; Tao, S.; Simonich, S. L. Heterogeneous reactions of particulate matter-bound PAHs and NPAHs with NO_3/N_2O_5, OH radicals, and O_3 under simulated long-range atmospheric transport conditions: reactivity and mutagenicity. *Environ. Sci. Technol.***2014,** *48*, (17), 10155-10164.